nuclear fusion

MHD analysis of high β_t disruptions in PBX

To cite this article: G.L. Jahns *et al* 1988 *Nucl. Fusion* **28** 881

MHD ANALYSIS OF HIGH $\langle\beta_t\rangle$ DISRUPTIONS IN PBX

G.L. JAHNS*, M.S. CHANCE, S.M. KAYE,
J. MANICKAM, H. TAKAHASHI, B. LeBLANC,
A.W. MORRIS**, M. REUSCH, S. SESNIC
Princeton Plasma Physics Laboratory,
Princeton University,
Princeton, New Jersey,
United States of America

ABSTRACT. Princeton Beta Experiment (PBX) discharges run at the lowest q and highest $\langle\beta_t\rangle$ always terminated in a hard disruption. The discharges, with $\langle\beta_t\rangle$ values of up to 5.5% and q-values down to 2.2, were obtained by employing large current ramps and large gas feed rates during neutral beam injection. Previous work has indicated that the achieved $\langle\beta_t\rangle$ values were consistent with the limit imposed by the n=1 ideal external kink with a conducting wall at b/a = 2. The authors of the paper investigate further the validity of ideal MHD theory in explaining the low q_ψ disruptions. In particular, the characteristics of the pre-disruption MHD activity in these low-q discharges, specifically the time-scale of growth and internal and external mode structures, are compared with those determined from theoretical calculations. The results of these comparisons indicate that non-ideal effects must be considered in order to obtain detailed agreement between theory and experiment.

1. INTRODUCTION

Theoretically, non-circular tokamak plasma operation enables access to the second regime of stability for both ballooning modes and internal kink modes, for moderate to large aspect ratios ($R/a \geq 4$) [1-3]. Therefore, the Poloidal Divertor Experiment (PDX) was converted to the Princeton Beta Experiment (PBX) by relocating a dome divertor coil to the vessel midplane so as to provide a means to form indented plasmas [4]. With this configuration and with up to 6 MW of perpendicular plus parallel neutral injection power, $\langle\beta_t\rangle$ values of up to 5.5% were attained in plasmas indented by 22% [5, 6]. Here, $\langle\beta_t\rangle$ is the volume averaged β calculated with the plasma pressure normalized to the volume averaged toroidal field pressure. The method of achieving these high $\langle\beta_t\rangle$ plasmas consisted of employing a large current ramp rate ($\dot{I}_p \geq 1.5\ \mathrm{MA\cdot s^{-1}}$) and strong gas puffing during the neutral injection phase. During the large current ramp period, internal m=1/n=1 modes, present during the early stages of neutral beam injection in these discharges, disappeared. Details of this *long sawtooth mode* of operation are discussed in Ref. [6].

During the *long sawtooth mode*, q_{MHD} decreased to values of ≤ 3.5 and sometimes to values as low as 2.1–2.5, corresponding to $q_{cyl} \approx 1.0$ and indicating plasma operation at extremely high average current density. Here, q_{MHD} is the q-value computed by a free-boundary equilibrium code at the 95% flux surface [4], and q_{cyl} is the q-value for a cylindrical discharge of equal cross-sectional area and current. A universal feature of the low q_{MHD} plasmas was a discharge terminating hard disruption during a period of increasing $\langle\beta_t\rangle$ and I_p. Values of $\langle\beta_t\rangle$ achieved just before the disruption at full beam power corresponded to $\langle\beta_t\rangle/(\mu_0 I_p/aB_t) = 2.0$–$2.5$, indicating that despite the high value of $\langle\beta_t\rangle$ ($\geq 4.5\%$) the plasmas still resided in the first regime of stability [7, 8]. A global stability calculation, based on the equilibrium configuration of these high $\langle\beta_t\rangle$ discharges, indicated that the value of $\langle\beta_t\rangle$ achieved just before disruption was consistent with the limit defined by the n=1 ideal external kink mode with a conducting wall at twice the plasma half-width [6].

The purpose of this paper is to investigate further the relevance of ideal MHD theory. This involves comparing theoretical and experimentally observed mode characteristics. To do this, the discharge stability must be determined, just as was done in the global stability calculation. An important first step in this process is the preparation of the discharge equilibrium. The equilibrium is calculated assuming that the total

* Permanent address: GA Technologies, Inc., San Diego, CA, USA.
** Permanent address: Balliol College, University of Oxford, UK.

plasma plus beam pressure profile is proportional to the electron pressure profile as determined from the 56-point Thomson scattering system. Then, the Grad–Shafranov equation is solved, the equilibrium solution being constrained by the experimental information on various parameters such as coil currents, plasma current, flux loop signals and diamagnetic loop output. With these constraints, the high $\langle\beta_t\rangle$ discharge of interest ($\langle\beta_t\rangle \simeq 5\%$) was best modelled by taking q(0) in the range of 0.8–0.9.

The results of the equilibrium calculation are then input into the PEST code [9] for determination of the discharge stability. The PEST code is a linear, ideal MHD spectral code, which uses the energy principle for determination of stability to small perturbations from an equilibrium condition. In the PEST calculation, the equilibrium is mapped onto a non-orthogonal magnetic field line co-ordinate system ($\tilde{\psi}$, θ), with 100 radial and 128 poloidal mesh points. For the low-q_ψ disruptive discharges being studied, the principal modes of interest are the low-n (=1) kink modes.

It was from these PEST global stability calculations that the ideal n=1 external kink was identified as the $\langle\beta_t\rangle$-limiting mechanism. This conclusion was based on the agreement between the measured and calculated $\langle\beta_t\rangle$, assuming q(0) = 0.89 and that a conducting wall resided at twice the plasma midplane half-width. The agreement between the measured and calculated $\langle\beta_t\rangle$ values is a necessary but by no means sufficient criterion for identifying the external kink as the instability that limits $\langle\beta_t\rangle$, especially since the placement of the wall is somewhat arbitrary. In fact, the placing of the wall at b/a = 2 and using q(0) = 0.89 was just one of the q(0), b/a combinations that gave agreement between the measured $\langle\beta_t\rangle$ and the limit given by the external kink; however, it is a combination that is consistent with the experimental constraints imposed upon the plasma equilibrium by the measurements. Other experimental results [10] also indicated the possible importance of invoking a cold mantle around the plasma to explain observations.

We attempt in this paper to provide a more precise comparison between the theoretical and experimental results by examining the actual mode structures and growth times. While the linear, ideal description is used as a jumping-off point for the comparison, the spirit of this paper is such as to ask what modifications to pure ideal theory must be made in order to bring the experiment and theory into agreement, and whether these modifications are reasonable. We show that ideal theory is only a zeroth-order description of the observed activity and that relaxation of the ideal constraints is necessary to bring about reasonable detailed agreement. While the relaxation of the ideal constraint may at first seem an ad hoc decision, it nevertheless serves a posteriori to illustrate effects that may be necessary to consider.

2. RESULTS

2.1. Mode activity before disruption

The *long sawtooth mode* discharges exhibit a period of little or no MHD activity up to a time of tens of milliseconds before the disruption. At that time, MHD activity, as measured by magnetic coils outside the plasma and by two soft X-ray detector arrays, was observed to increase slowly at first and then to undergo a rapid growth. An example of the final, approximately exponential growth of the precursor activity is presented in Fig. 1, which shows the $\dot{B}_\theta$ signal as measured by a magnetic pickup loop on the plasma midplane, approximately 20 cm outside the plasma edge. The growth time of the mode is 120 μs for this case. Just before the final growth, the mode had a characteristic frequency of 9 kHz and a peak amplitude of 6.5 G ($\delta B_\theta/B_\theta \simeq 0.3\%$) at the coil. Just before the disruption, the discharge had the following characteristics: I_p = 520 kA, B_t = 0.9 T, indentation = 20%, $\bar{n}_e = 5 \times 10^{13}$ cm^{-3}, q_{MHD} = 2.9, P_{inj} = 4.5 MW, $D^0 \rightarrow H^+$, and $\langle\beta_t\rangle$ = 5.0%. For this

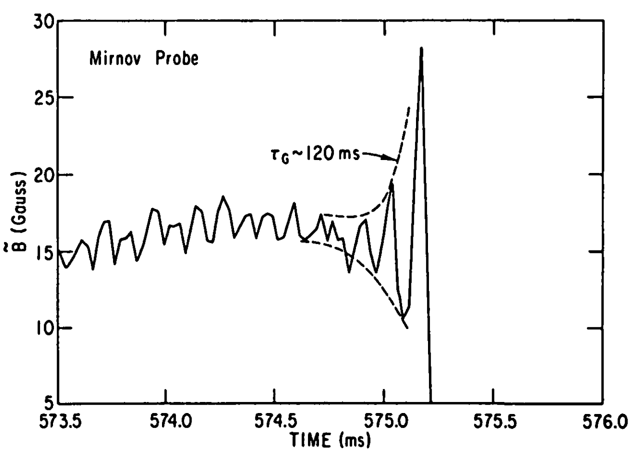

FIG. 1. Expanded time-scale of the integrated magnetic signal for a discharge with zero delay, showing the final, approximately exponential growth of the disruption precursor mode. The dashed line schematically indicates the approximate exponential growth of the oscillation envelope.

discharge, the precursor mode led directly into the growth phase of the plasma disruption at 574.8 ms. However, this was not always the case; often the precursor growth led to an internal disruption, followed by a period of several milliseconds, typified by little or no oscillatory magnetic activity, between the internal and final disruption. The soft X-ray structure of the internal disruption resembled a sawtooth, consisting of a central collapse and an inversion approximately at the q = 1 surface. However, there were differences between the internal disruption and the sawteeth; this will be discussed in a future report. It is important to note that $\langle\beta_t\rangle$, in a given shot, decreased with the first internal disruption and never completely recovered. Thus, it was the initial internal disruption and not the final disruption (if these disruptions were separate) that was the $\langle\beta\rangle$-limiting process. The edge oscillations and the mode growth, as seen on the Mirnov coils, were often accompanied by oscillations and growth of m=1/n=1 internal modes, as seen on the soft X-ray array. At first, this result seems inconsistent with a limit imposed by a surface mode. This apparent paradox will be resolved in Section 2.4, where it is shown that an n=1 external kink mode drives a large m=1 component for certain conditions in PBX discharges.

2.2. Probability of disruption

As mentioned, a universal feature of all plasmas with $q_{MHD} \leq 3.5$ and with indentations of $\geq 5\%$ is a discharge limiting disruption. This is true for all discharges, regardless of the ratio of $\langle\beta_t\rangle/(\mu_0 I_p/aB_t)$, i.e. regardless of how close the plasma is to the first regime limit. In this section we examine the probability that a discharge will disrupt as a function of q_ψ. The motivation for this is twofold. First, the results will serve as a quantitative indicator of discharge survivability within the operating space that leads to high $\langle\beta_t\rangle$. Second, the way in which the disruption probability changes as a function of q_ψ will serve as an indication of the type of mode responsible for the disruption.

Figure 2 is a histogram of the number of discharge disruptions as a function of the q_{MHD} at which the discharges disrupted, grouped in bins of $\Delta q_{MHD} = 0.1$. The data are taken from a subset of PBX discharges that attempted to reach low q. Thus, while the histogram is representative of discharges with $q_{MHD} \leq 3.5$, it contains little information for discharges with q_{MHD} higher than this value. Since *all* the discharges with $q_{MHD} \leq 3.5$ disrupt, the figure reflects the probability that a plasma with a strong current ramp will achieve a particular q_{MHD}. The sharp peak in the number of

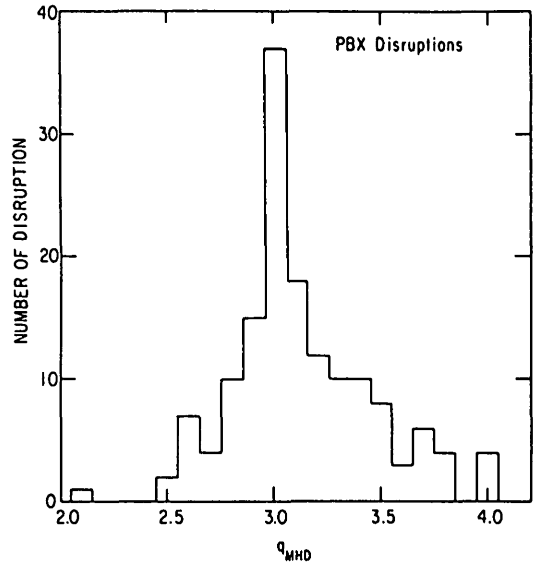

FIG. 2. Probability of disruption as a function of q_{MHD} in bins of $\Delta q_{MHD} = 0.1$ for PBX discharges. The distribution of discharges used to produce this figure is weighted towards lower q_{MHD} (≤ 4).

disruptions at $q_{MHD} \approx 3.0$ indicates the difficulty in attaining low q; it also strongly suggests that edge q is an important parameter for plasma stability. The skewing of the distribution towards higher q_{MHD} indicates that relatively few discharges survive to the lowest q-values (≤ 3). While some shots survived to q ~ 2.5, only one shot lasted to lower q; this is in contrast to high $\langle\beta_t\rangle$ circular discharges on PDX where $q_{MHD} \approx q_{cyl} = 2.0$ were routinely achieved. However, as previously mentioned, many $q_{MHD} \leq 3.0$ PBX discharges had equivalent q_{cyl} values of approximately one, reflecting the much greater current carrying capability of shaped plasmas. A brief discussion of whether it is the current or $\langle\beta_t\rangle$ that predominantly drives the disruption is given in Section 3.

Figure 2 includes many data for which there was a small delay between the internal disruption and the final disruption, as discussed above. This means that $q_{MHD} = 3.0$ is a good predictor of the occurrence of an internal disruption; also, it presents strong evidence that the internal disruption is driven by a global mode.

2.3. Time-scales

As stated previously, the process limiting $\langle\beta_t\rangle$ at this low q-value is believed to be the ideal n=1 external kink mode [6]. A test of the validity of ideal MHD theory can be made by examining the main characteristics of the disruption precursor mode — the mode believed to be the external kink. The first characteristic to be studied is the time-scale on which the mode grows and leads to the disruption; for the second characteristic, a comparison is made between the measured internal/external mode structures and those theoretically predicted.

The estimated average time-scale of the final growth for the mode shown in Fig. 1 is 120 μs. Typically, the growth times of the disruption precursor range from tens of microseconds to ≤ 2 ms. Typical ideal time-scales are given by the poloidal Alfvén time, which is

$$\tau_A = \rho^{1/2} a / B_\theta \approx 2\ \mu s$$

although, as pointed out by Wesson [11], the time-scales for ideal mode growth can be an order of magnitude higher, even with no conducting wall, for $m-nq \approx 0$. A typical resistive time-scale is

$$\tau = \left(\tau_R^{0.6} \tau_A^{0.4}\right) \simeq 1\ \text{ms}$$

where τ_R is the resistive skin time. The range of observed growth times is generally bounded from below by the ideal time-scale and from above by the resistive time-scale. The PEST stability calculation does yield mode growth times; however, the computed values show a great deal of variability. For instance, when q(0) was varied from 0.85 to 0.95 to study the sensitivity of the $\langle\beta_t\rangle$ limit and mode growth to variations in this parameter, the calculated growth rates varied by a factor of four to five, although they still remained in the ideal range (few to tens of microseconds). Because of the sensitivity to q(0) and because the growth rates determined by PEST are linear ones, we do not believe it to be relevant to make direct comparisons between the PEST growth rates and those observed experimentally.

What is of importance is to ask whether there are any effects within the framework of ideal theory that can cause a slowing-down of mode growth to yield the range of growth times observed. Some of these effects include the presence of a stabilizing conducting wall (which was found to be necessary in the PEST calculation to bring the measured and theoretical $\langle\beta_t\rangle$ limit values into agreement [6]). Another effect that would slow down the mode growth rate is the presence of a pressureless plasma mantle in the region exterior to the plasma [12]. Independent of these considerations, a slow mode growth can occur naturally; it can be explained by the observation that the onset of the instability usually occurs as a result of plasma parameters, such as the current or pressure, evolving in time through the marginal state for the instability. Calculations taking this effect into account show that the mode growth rate is not simply a pure exponential growth but one which increases with time, and that it is a function of both the slow evolution time of the equilibrium and the fast time usually associated with the mode (the poloidal Alfvén time in the ideal case). A rough estimate of this effect can be obtained as follows. Assume that the mode equation can be modelled as:

$$\frac{d^2\xi}{d\tau^2} + [F_c - F(t)]\xi = 0$$

where F_c is the critical threshold of the mode and F(t) is the evolving equilbrium state. If $F(t) \cong F_c + t\dot{F}(t)$, we have

$$\frac{d^2\xi}{d\tau^2} - \tau\xi = 0$$

where $\tau = \dot{F}^{1/3}t$, i.e. Airy's equation with the solution

$$\xi = \alpha \mathrm{Ai}(\tau) + \beta \mathrm{Bi}(\tau)$$

A characteristic time for the mode is therefore

$$\tau_c = \dot{F}^{-1/3}$$

A heuristic estimate of τ_c for the external kink mode can be made if we write the usual dispersion relation for the straight circular cylindrical model with constant current and wall at r = b in the form (see Ref. [13])

$$\frac{d^2\xi}{dt^2} - \frac{2}{\tau_A^2}(m - nq)\left(1 - \frac{m - nq}{1 - \left(\frac{a}{b}\right)^{2m}}\right)\xi = 0$$

where we replaced $-\omega^2$ by d^2/dt^2; τ_A, the hydromagnetic or poloidal Alfvén time, is defined as before, and ξ is the displacement. If the total plasma current is increasing in time through the marginal state, then

$$m - nq \simeq -n\dot{q}t = nqt\ \dot{I}/I$$

so that for the external kink

$$\tau_c = \tau_A \left(\frac{1}{2nq}\frac{\tau_e}{\tau_A}\right)^{1/3} = \left(\frac{1}{2nq}\tau_e\right)^{1/3}\tau_A^{2/3}$$

i.e. a hybrid time between the poloidal Alfvén time and the evolution time ($\tau_e \equiv I/\dot{I}$) of the equilibrium. In this case, the position of the wall does not enter. Applying this to our typical PBX parameters, where n=1, $q_{MHD} \approx 3$, $\tau_e \approx 0.35$ s and $\tau_A \approx 2$ μs, we find that the characteristic time τ_c is approximately 62 μs.

The mode growth time, defined by $\tau_g \equiv (d \ln \xi/dt)^{-1}$, differs from τ_c and decreases with time. After one characteristic time, we can approximate $\xi \sim \mathrm{Bi}(t)$ and find that $\tau_g = \tau_c$ at $t = \tau_c$. Moreover, the time taken for τ_g to be $\sim \tau_A$ is roughly the equilibrium evolution time, τ_e (usually $\gg \tau_c$), before which the plasma discharge usually terminates. The situation is, therefore, that $\tau_g > \tau_c$ before τ_c, $\tau_g < \tau_c$ after τ_c, and usually $\tau_g \gg \tau_A$. In this model, $\tau_g \rightarrow \infty$ at $t = 0$, but in reality the upper limit could be determined by background plasma fluctuations.

The value of τ_c of 60 μs obtained here from the — albeit crude — cylindrical model is still smaller than a good share of the observed growth times, so that either the plasma disrupts before $t = \tau_c$ when τ_g is calculated or other effects slowing down the mode growth must also play a role (as discussed in the next section).

2.4. Mode structures

As described in Section 1, the PEST calculation is used to determine the discharge stability to small perturbations from an equilibrium condition. Since the entire discharge equilibrium is tested for stability, both internal and external mode structures may result. We do not a priori restrict ourselves to considering either internal or external modes. For the n=1 modes of interest here, the results of a PEST analysis are displayed in Fig. 3. Figure 3(a) shows a projection of the plasma displacement onto the x-z plane at a particular toroidal angle ($\Phi = 0$); as Φ is increased, the pattern rotates and returns to this configuration at $\Phi = 2\pi$. The arrows indicate the direction and the length is proportional to the amplitude of the displacement. The mode structure is Fourier analysed and the radial variation of the different harmonics is presented in Fig. 3(b). This shows only the radial components of the displacement vector, $\xi_\psi = r\xi_r$, and demonstrates the dominance of the m=1 component. This analysis is for a free-boundary case and hence the radial displacement at the plasma edge, $\Psi \cong 1$, is finite, However, the different harmonics tend to cancel out, as can be seen in the arrow plot, and the dominant contributions are due to the m=1 and m=2 modes inside the plasma.

A large m=1 mode is observed experimentally, as shown in Fig. 4. Plotted in the figure are the relative amplitudes (a) and phases (b) of the internal fluctuations of the disruption precursor mode, just before the disruption itself, as seen by the horizontally viewing soft X-ray array. The amplitudes and phases are plotted as functions of Z, with Z being the distance from the midplane to the intersection point of the vertical axis at R = 145 cm and the X-ray detector sight line (the major radius of the discharge was R_0 = 144 cm). The precursor mode in this case, with a frequency of 17.5 kHz, shows a maximum relative

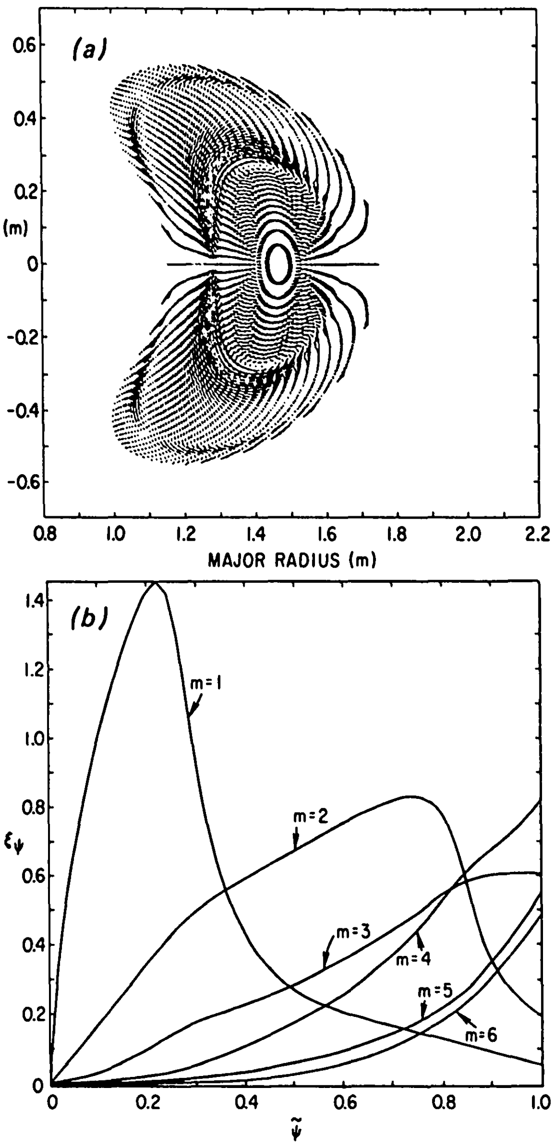

FIG. 3. Eigenmode structure of the displacement from the PEST analysis. (a) Projection of the displacement vector onto the x–z plane at a particular toroidal angle. (b) Radial variation of the eigenmode harmonics. Plotted are the radial displacement vectors, $\xi_\psi = r\xi_r$, as a function of the toroidal flux co-ordinate $\tilde{\psi}$.

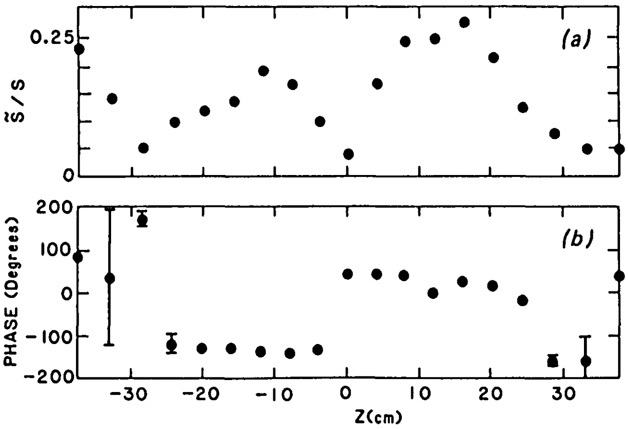

FIG. 4. Relative amplitude (a) and phase (b) of the disruption precursor mode as measured by the horizontally viewing soft X-ray array. The measured signal is a line integral.

amplitude of 20–25% at Z = ±12 cm (Fig. 4(a)), the approximate location of the q = 1 surface as determined from the equilibrium calculation. The phase plot (Fig. 4(b)) indicates a ~180° phase jump across the centre of the plasma, indicative of a clear m = 1 mode at this frequency. The quality of the data at large negative Z is poor, and this is reflected by the large error bars in the relative phases for Z ≤ -25 cm.

The PEST stability analysis has been modified recently to permit a computation of the expected magnetic signals at various points in the vacuum vessel so that these signals can be compared with the measured ones. To minimize the danger involved in a comparison of the linearized PEST modes with the observed modes, which may have significant non-linearities, the time point of comparison is just after the onset of growth leading to the disruption. The comparison is shown in Fig. 5. The measured signals are plotted in Fig. 5(a) for the usable Mirnov coils. Plotted are the time integrated signals $\tilde{B}_\theta$ just before the disruption. For orientation, coils 1 through 12 form a poloidal array at one toroidal location, with coils 8 and 2 being on the inside and outside midplane, respectively. Coil pairs (13, 14) and (15, 16) are also midplane in/out pairs, but they are displaced 90° and 180° toroidally from the (8, 2) pair.

The perturbed signal, as calculated by PEST, is plotted as a function of toroidal angle Φ in Fig. 5(b). Note that the abscissae in Figs 5(a) and 5(b) are assumed to be related through a simple toroidal rotation of an n = 1 mode stationary in the plasma frame. The signal was calculated for an n = 1 mode with the conducting wall at infinity. Moving the wall into

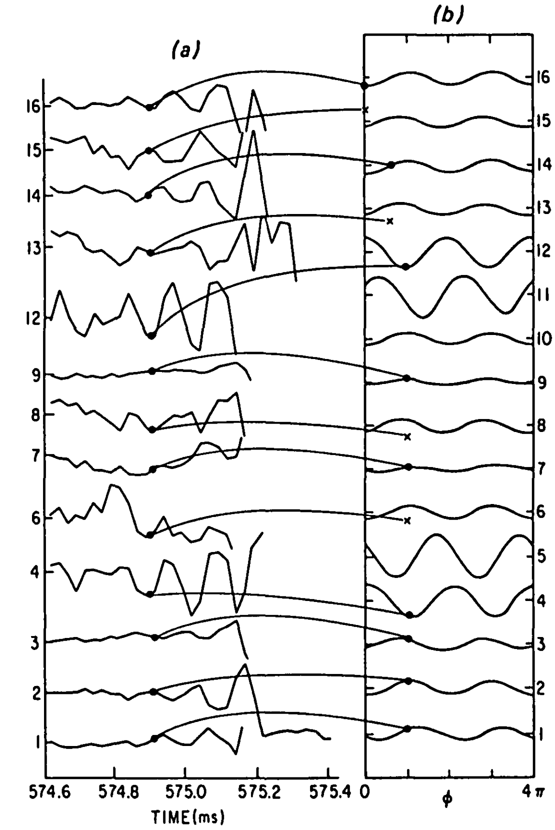

FIG. 5. Comparison of the time integrated magnetic signals measured experimentally (a) and calculated theoretically (b) for an n=1 mode. The abscissae (time and toroidal angle) are related through simple toroidal rotation, as described in the text.

b/a = 2 has little effect on the relative phases of the magnetic perturbations. The lines connecting the signals in Figs 5(a) and 5(b) merely help guide the eye in translating the instantaneous amplitude and phase of the measured signal for comparison with the theoretical value at the appropriate toroidal angle.

There are several things to note from this comparison. First, the relative amplitudes of the theoretical signals, in general, agree quite well with those of the measured signals. Additionally, the phases of coils 1 through 4 as well as coils 7, 9, 12, 14 and 16 also show good agreement between experiment and theory. The coils for which the phases disagree are numbers 6, 8, 13 and 15 (denoted by × in Fig. 5(b)), all of which are located on the inner wall. For these coils, the phase disagreement between theory and experiment is about 180°; thus, while we expect an even poloidal mode structure from ideal calculations, we observe an odd mode, more specifically an m = 3 mode.

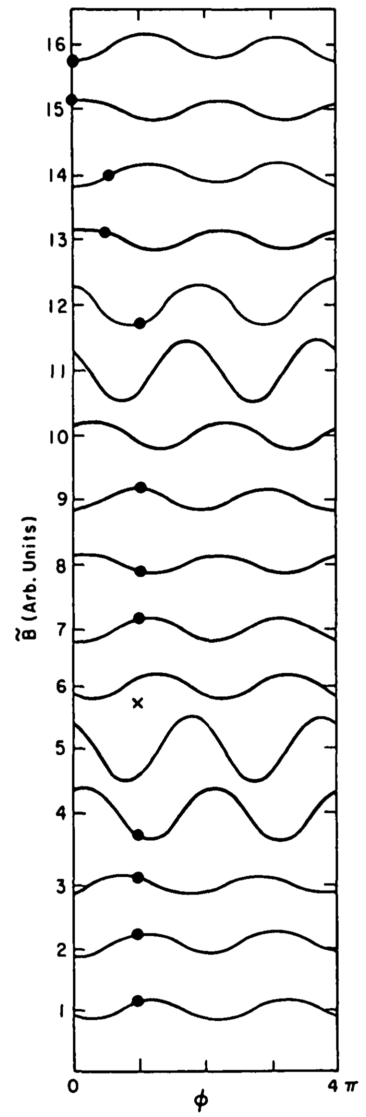

FIG. 6. Same as Fig. 5(b), with $\delta B_3 \simeq \delta B_4$.

The discrepancy between the observed and expected phases points to the inadequacy of ideal theory in this case. In the ideal MHD limit, since $\delta B_m \propto (m - nq)\xi_m$ (where δB_m and ξ_m are the radial perturbed magnetic and fluid displacement amplitudes of the m-th Fourier component), the magnetic perturbation of the m=3 component would be close to zero at the plasma vacuum interface since $q_{MHD} \simeq 2.93$ for this discharge. Since the radial magnetic field is continuous across the interface and an m=3 component is clearly observed in the vacuum region, there must be some mechanism by which this component can be supported. One such mechanism is the presence of a cool, resistive external plasma mantle. To model the possible effect of such a resistive mantle, we increased the value of ξ_3 in the simulation so that, arbitrarily, $\delta B_3 \simeq \delta B_4$. This somewhat ad hoc treatment should be viewed as a 'Gedanken experiment' in which we ask what are the possible modifications to the pure ideal theory that are necessary to bring experiment and theory into agreement. The consideration of a cool, resistive plasma mantle, found to be potentially important for explaining DIII data [10], is certainly one reasonable modification. The recomputed magnetic perturbation signals and comparisons are shown in Fig. 6, where it is seen that now all of the loops, except for loop number 6, show phase agreement between theory and experiment. Loop 6, as well as the other loops located on the inner wall, is close to metal conductors, which are not accounted for in the theory. This effect of resistivity is reminiscent of the kink-tearing calculation of Pogutse [12], which could also account for a significant decrease in the growth of the mode below the pure infinite resistive vacuum model.

From the observations by the soft X-ray array and the Mirnov coils, it can be concluded that the MHD behaviour near the disruption is adequately described by external kink modes with significant m=1/n=1 structure inside the plasma. The magnitude of this component may depend on q(0), the location of the q = 1 surface, and possibly the q-profile at q = 1. This hypothesis is consistent not only with the mode structure but also with the observed dependence of the strength of the central m=1/n=1 component on small changes in discharge parameters near the time of the disruption. An example of this is that discharges that survive down to lower q_{MHD} have a smaller m=1/n=1 amplitude just before disruption. Although measurements of the significant parameter q(0) are not available at present, this hypothesis, supported by theoretical analysis, can indicate possible paths to improve MHD behaviour and to stabilize the hard disruption.

3. SUMMARY AND DISCUSSION

The $\langle\beta_t\rangle$ limit in PBX low q_{MHD} plasmas is manifest as a discharge limiting disruption, in either a two-step disruption (internal disruption followed quickly by a total disruption) or an immediate disruption. The disruption follows a period of up to 150 ms of MHD quiescent behaviour, interrupted only by small-amplitude magnetic and soft X-ray activity, growing slowly over approximately 20 ms before the disruption and culminating in a much more rapid exponential growth, with growth times of the order of 10 μs to several milliseconds.

This activity was observed to be m = 1/n = 1 internally by the soft X-ray array and m = 3/n = 1 by the Mirnov coils. Previous work suggested that the n = 1 ideal external kink mode was responsible for the $\langle\beta_t\rangle$ limit in these low-q discharges [6]. Here, an effort was made to compare the characteristics of the observed pre-disruption MHD activity with those expected from ideal theory. The characteristics studied included time-scales and mode structures of the internal and external activity.

The comparisons between theory and experiment were performed primarily with calculated results from the PEST stability code, which is based exclusively on linear, ideal theory. Because of these limitations and because of the uncertainties in key input parameters to the code, care must be taken concerning what code output to focus on. Observationally, the time-scales for mode growth varied from microseconds to milliseconds. While the PEST calculations indicated growth times of a few microseconds to tens of microseconds, these values were found to be extremely sensitive to input q(0), varying by a factor of four to five as q(0) was varied from 0.85 to 0.95. In addition, the PEST growth time is a linear value. Therefore, the growth times as calculated by PEST are not indicative of the true experimental environment. An attempt to impose some real quasi-linear modifications of the growth time was made by taking into account the way in which the plasma evolves through the state of marginal stability. This consideration allows a large range of growth times (up to the ≈ 100 μs level) to be accounted for within the framework of ideal theory.

The stability analysis results indicate that the eigenmode structure of the ideal n = 1 kink exhibits a predominantly m = 1 structure internally, and this is borne out observationally. For the poloidal structure of the external magnetic signals there is not such a good agreement between theory and experiment. The amplitudes of the various coil signals do show good agreement, but the poloidal mode structure does not. The reason for this is the ideal constraint, which suppresses the amplitude of the m = 3/n = 1 component (theoretically) near the plasma edge for this $q_\psi \simeq 3$ discharge. Since an m = 3 component is observed, it is clear that this ideal constraint is not valid, and one way to lift this constraint is to allow for a resistive plasma mantle wich can support a finite m = 3 component. Using this approach, the phases can be brought into agreement when the amplitude of the m = 3 component is taken to be of the same size as the amplitude of the m = 4 component.

To determine whether it is the current or $\langle\beta_t\rangle$, or both, that predominantly drives these low q_ψ disruptions, a global stability analysis of a discharge with $q_\psi = 3.1$ and $\langle\beta_t\rangle = 2.9\%$ was performed in the same manner as the analysis presented in Ref. [6] for the low q_ψ high $\langle\beta_t\rangle$ discharge. The results of the PEST analysis for the lower $\langle\beta_t\rangle$ case indicated that this plasma also was ideal n = 1 kink unstable, with the wall at infinity, and could be stabilized only when the wall was brought in to b/a = 1.5. The calculated mode structures of the higher and lower $\langle\beta_t\rangle$ discharges were similar, although the lower $\langle\beta_t\rangle$ discharges did exhibit, both observationally and from the PEST results, an internal m = 1 component that was more dominant in both amplitude and extent than that of the higher $\langle\beta_t\rangle$ discharge. The dominance of the m = 1 component, which may be responsible for the more unstable nature of the lower $\langle\beta_t\rangle$ low q_ψ discharges, depends on the detailed characteristics and evolution of the plasma current and pressure profiles. In some cases, the profile characteristics are such that the instability, and thus the ultimate disruption, is delayed until a high $\langle\beta_t\rangle$ is reached.

In conclusion, pure ideal MHD theory provides a reasonable guideline for global stability analysis and for the general conclusion that the n = 1 external kink is the mechanism limiting $\langle\beta_t\rangle$ in the low-q PBX discharges, regardless of the value of $\langle\beta_t\rangle$. This is consistent with using the Troyon–Sykes beta limit as a useful guide for stability thresholds, since this limit is also based on ideal MHD simulations. However, the ideal theory alone leads to discrepancies between the experimental results and the theoretical predictions regarding the precise characteristics of the MHD activity leading to the disruption. Imposing effects outside the scope of ideal MHD theory is necessary in order to bring about more detailed agreement at this level.

ACKNOWLEDGEMENTS

The authors would like to thank K. Bol, M. Okabayashi and the rest of the PBX Group for support during the course of this work. They also gratefully acknowledge discussions with K. McGuire and D. Buchenauer. A portion of this work was carried out while one of the authors (G.L.J.) was visiting PPPL.

The PBX project was supported by the United States Department of Energy, under Contract No. DE-AC02-76-CHO-3073.

REFERENCES

[1] CHANCE, M., JARDIN, S., STIX, T., Phys. Rev. Lett. **51** (1983) 1963.

[2] MANICKAM, J., GRIMM, R., OKABAYASHI, M., Phys. Rev. Lett. **51** (1983) 1959.

[3] GRIMM, R., CHANCE, M., TODD, A., et al. Nucl. Fusion **25** (1985) 805.

[4] OKABAYASHI, M., BEIERSDORFER, P., BOL, K., et al., in Plasma Physics and Controlled Nuclear Fusion Research 1984 (Proc. 10th Int. Conf. London, 1984), Vol. 1, IAEA, Vienna (1985) 229.

[5] KAITA, R., BOL, K., COUTURE, P., et al., in Controlled Fusion and Plasma Heating (Proc. 13th Eur. Conf. Schliersee, 1986), Vol. 28, European Physical Society (1986) 1319.

[6] BOL, K., BUCHENAUER, D., CHANCE, M., et al., Phys. Rev. Lett. **57** (1986) 1891.

[7] TROYON, F., GRUBER, J., SAURENMANN, H., SEMENZATO, S., SUCCI, S., Plasma Phys. Controll. Fusion **26** (1984) 209.

[8] SYKES, A., TURNER, M., PATEL, S., in Controlled Fusion and Plasma Physics (Proc. 11th Eur. Conf. Aachen, 1983), Vol. 7D, Part II, European Physical Society (1983) 363.

[9] GRIMM, R., GREENE, J., JOHNSON, J., Methods Comput. Phys. **16** (1976) 253.

[10] STAMBAUGH, R.D., MOORE, R.W., BERNARD, L.C., et al., in Plasma Physics and Controlled Nuclear Fusion Research 1984 (Proc. Int. Conf. London, 1984), Vol. 1, IAEA, Vienna (1985) 217.

[11] WESSON, J., Nucl. Fusion **18** (1978) 87.

[12] POGUTSE, O.P., Kink and Tearing Mode Instabilities in a Tokamak, Rep. PPPL-TRANS-121, Princeton Plasma Physics Laboratory, Princeton University, NJ (1977).

[13] SHAFRANOV, V., Sov. Phys.-Tech. Phys. **15** (1970) 175.

(Manuscript received 5 February 1987
Final manuscript received 1 February 1988)